World Conference on Timber Engineering Oslo 2023

NUMERICAL EXAMINATION OF THE BEHAVIOUR OF DOWEL LAMINATED TIMBER ELEMENTS UTILISING COMPRESSED WOOD DOWELS

Conan O'Ceallaigh[1], Annette M. Harte[2], Patrick J. McGetrick[3]

ABSTRACT: This study examines the use of finite element software to model the failure behaviour of a dowel laminated timber (DLT) beam which is connected with the use of modified or compressed wood dowels. The numerical model is validated against experimental results and a parametric study is carried out to further examine the influence of dowel diameter and dowel spacing on the load-displacement behaviour of the DLT beams. The numerical model is shown to accurately simulate the ultimate failure load and the stiffness of the DLT beams. The influence of dowel diameter and dowel spacing are presented. The results demonstrate that DLT technology can be used to further improve the environmental performance of timber construction by replacing the use of adhesive which is commonly used when manufacturing laminated engineered wood products.

KEYWORDS: Compressed wood dowels; Dowel Laminated Timber (DLT); Engineered Wood Products (EWPs); Foundation zone, Numerical modelling; Parametric study

1 INTRODUCTION

In recent years, there has been an increased focus on the environmental impacts of construction and a movement towards more sustainable construction products. Dowel Laminated Timber (DLT) products are one such Engineered Wood Product (EWP) that can carry significant structural loads with a limited carbon footprint. The DLT process typically involves the use of hardwood dowels positioned within drilled holes to form a tight fit connection between adjacent laminations as shown in Figure 1. The use of such technology has been successfully utilised to form DLT panels and beams using a variety of different timber species [1–3]. This technology ultimately reduces the use of adhesives in EWPs and further improves the environmental credentials. The efficiency of the connection is reduced when compared to adhesively bonded EWPs and as such, it is important to understand the parameters that affect the strength and stiffness of such connections and the ultimate strength and stiffness of the developed DLT product.

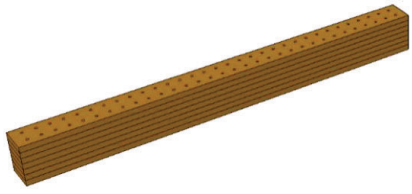

Figure 1: *Typical dowel laminated timber (DLT) beam connected with hardwood timber dowels.*

In this study, the use of compressed timber dowels is explored as a potential alternative to hardwood dowels. Compressed wood (CW) dowels are made from softwoods, which are compressed under heat and pressure which enhances their structural properties, and have been shown to have excellent properties when used in timber connections [4,5]. DLT members are manufactured and tested in accordance with EN 408 [6] to determine their ultimate failure behaviour and stiffness. The experimental results are utilised to validate a numerical model, which is then used in a parametric study to examine the influence of dowel diameter and dowel spacing on the structural response of the DLT members.

2 DOWEL LAMINATED TIMBER

2.1 INTRODUCTION

The use of dowel laminated technology has been the subject of a number of studies in recent years as an alternative to glued laminating technology to further improve the environmental performance of EWPs [1–3,7–12]. There have been significant advances in this technology and a number of commercial products are available and in use in several large timber structures across the world [1,13]. The DLT members utilised in this study were manufactured in the Timber Engineering Research Group (TERG) laboratory at the University of Galway. The timber substrate used is Sitka spruce, grown in Ireland, which is characterised as a fast-grown timber with a C16 structural grade. The CW dowels are

[1] Conan O'Ceallaigh, Timber Engineering Research Group, University of Galway, conan.oceallaigh@universityofgalway.ie
[2] Annette M. Harte, Timber Engineering Research Group, University of Galway, annette.harte@universityofgalway.ie
[3] Patrick J. McGetrick, Timber Engineering Research Group, University of Galway, patrick.mcgetrick@universityofgalway.ie

https://doi.org/10.52202/069179-0030

manufactured from Sitka spruce which has undergone a process known as thermo-mechanical compression which reduces the void space within the lumen between the cell walls increasing the density significantly and improving many structural properties of the timber. These are dicussed further in the following sections.

2.2 TIMBER & COMPRESSED WOOD DOWELS

For the purpose of this study, Sitka spruce, grown in Ireland, is the primary material under investigation. From a structural point of view, this species commonly achieves a structural grade of C16 due to the climatic conditions in which it grows. The standard EN 338 [17] provides a mean value of 8000 MPa for the elastic modulus of C16 timber in the longitudinal direction which is used as the primary substrate for the DLT members in this study. Typically, hardwood dowels have been used in the manufacture of DLT products, however, in this study, CW dowels are used. CW is a type of modified wood material that has been shown to have superior structural properties to natural timber and has proved to be an environmentally friendly alternative to metallic fasteners in timber connections [4,19–22]. The CW used in this study was produced by a process of thermo-mechanical compression of sitka spruce softwood timber to increase its density, strength, stiffness, hardness and to reduce its porosity [23,24].

CW in the form of dowels has demonstrated good properties when tested in shear and when compared with other standard hardwood dowels [24]. The modification process requires the application of pressure at a specific temperature. As the temperature of the timber increases, it may be easily compressed reducing the void space between the cell walls, increasing the density significantly and improving many structural properties of the timber. As the density of the timber is increased, a proportional improvement in stiffness, yield load and maximum load is expected. However, in contrast, the plastic modulus has been shown to decrease in some species [25]. The CW, with enhanced structural properties compared to standard hardwood dowel, also has a spring-back or shape-recovery property that means it will expand over time resulting in a tight fit connection that may be a beneficial characteristic in many structural timber engineering applications, particularly DLT beams and panels [26].

2.3 BEAM GEOMETRY

The beam geometry under investigation in this study is presented in Figure 2. The beam comprises three Sitka spruce timber laminations measuring 1140 mm in length and a cross-section of 20 mm x 60 mm. The three timber laminations are combined to form a final cross-section of 60 mm x 60 mm and a length of 1140 mm. The specimen geometry was chosen based on the criteria for the bending test specified in EN 408 [6]. The manufactured DLT members in Figure 2 are manufactured using CW dowels with a diameter of 10 mm and the dowel spacing of 100 mm. A total of 3 DLT members were manufactured with the same dimensions, dowel diameter and dowel spacing.

Figure 2: *Manufactured DLT members utilising 10mm diameter dowels and the dowel spacing of 100mm.*

3 EXPERIMENTAL TESTING

The DLT timber specimens were subjected to experimental testing under four-point bending in accordance with EN 408 [6]. This test standard specifies four-point bending over a test span of 18 times the specimen depth. As a result, the test specimen is supported over a test span of 1080 mm with point loads at 360 mm from each support. Steel plates (60 mm x 30 mm x 10 mm) are positioned at the support points and load points as specified by EN 408 [6]. As seen in Figure 3, the midspan of each beam is represented by a red dotted line and it is at this location that the global vertical displacement of the beam is determined for a given load until failure occurs. This is also the line of symmetry used when modelling the DLT member using finite element software discussed later.

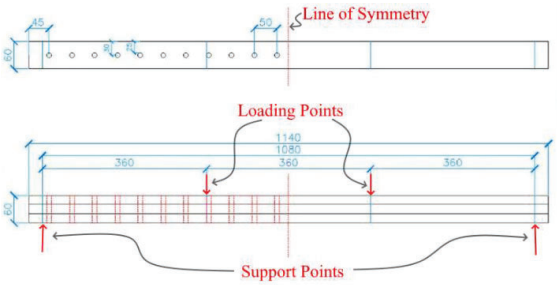

Figure 3: *DLT geometry for the 10mm diameter dowels and the dowel spacing of 50mm (DLT-D10-S50). Dimensions in mm.*

The load-displacement behaviour of each DLT member can be seen in Figure 4. It can be seen that the load-displacement behaviour of each DLT member is relatively similar and is characterised as linear elastic until brittle failure occurs. There are a series of small instances of failure whereby the load drops and is recovered until the ultimate failure occurs. In Figure 4, a line indicated as 'Glulam' represents the theoretical stiffness of a glued laminated beam with an elastic modulus of 9200 N/mm^2 to allow for comparison with the stiffness of the DLT members. It is clear that the stiffness of the DLT members is much less than that of the glued laminated member.

https://doi.org/10.52202/069179-0030

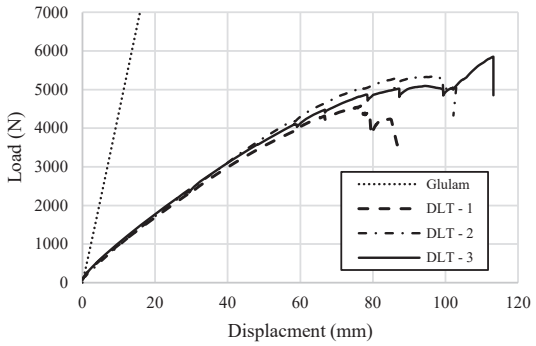

Figure 4: *Load-displacement behaviour of the DLT members*

A summary of the results is presented in Table 1. The results show that significant loads can be achieved for such DLT members connected solely with CW dowels. The maximum load (F_{max}) ranged from 4.57 – 5.85 kN with a mean value of 5.26 kN and a standard deviation of 0.6 kN. The corresponding ultimate displacement ranged from 76.6 - 113.2 mm with a mean value of 94.5 mm and a standard deviation of 18.3 mm. This magnitude of deflection indicates that the stiffness of the DLT members is relatively low. This is clear from the load-displacement curves presented in Figure 4 where the DLT members can be compared to an equivalent glued laminated member of similar dimensions. The only difference is the efficiency of the connection between the laminations of the elements. The adhesive used in glued laminated beams is quite efficient at transferring load between laminations and results in a fully composite beam. The dowels in the DLT are less efficient at transferring this load and as a result, reduced stiffness is observed.

The stiffness results from the tests are presented in Table 1. The stiffness ranges from 1520 – 1588 N/mm^2 with a mean value of 1548 N/mm^2 and a standard deviation of 35.3 N/mm^2. It should be noted that these results are also dependent on the dowel diameter and spacing used and there is a significant opportunity to optimise the dowel configuration to improve the strength and stiffness.

Table 1: *Experimental results of testing on DLT members*

Member	F_{max} (kN)	U_{max} (mm)	Stiffness (N/mm^2)
DLT-1	4.57	76.6	1520
DLT-2	5.34	93.8	1588
DLT-3	5.85	113.2	1537
Mean	5.26	94.5	1548
Std. Dev.	0.6	18.3	35.3

The typical failure behaviour of the DLT beams is shown in Figure 5. The most significant failure behaviour observed was a brittle failure of the timber along the bottom tensile laminate of the DLT beams. This occurred under the load point between the shear-free region of the beam. It is also clear from Figure 5 that significant interlaminar slip occurred in each beam between the load points and the support points. This can be seen at the end of the beam where a stepped profile can be observed.

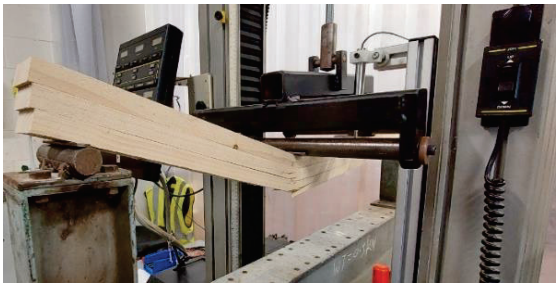

Figure 5: *Failure behaviour of DLT member (DLT - 2)*

To further examine this interlaminar slip, each specimen was split along the middle of the beam through the axis of the dowels to observe the behaviour at the dowel-timber interaction post-failure. An example of this can be seen in Figure 6. It is clear that significant dowel-timber embedment has occurred, particularly in the high-shear areas of each beam.

Figure 6: *Interlaminar slip, stepped profile and dowel-timber embedment.*

4 FINITE ELEMENT MODEL

4.1 MODEL DEVELOPMENT

A three-dimensional finite element model is developed, incorporating a UMAT subroutine to determine the total strain and associated damage experienced in DLT timber members when subjected to a structural load. The model is validated based on the results of the experimental test. As seen in Figure 7, the model utilises half symmetry to reduce the number of elements and computational time to solve the model. A symmetry boundary condition at the midspan is used to achieve this.

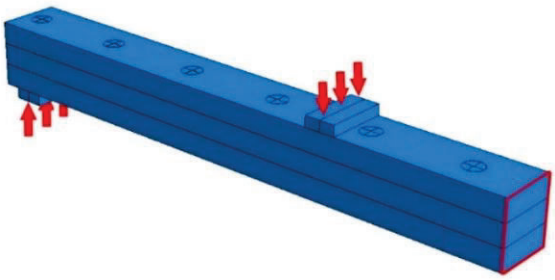

Figure 7: *Numerical model geometry subjected to four-point bending utilising half symmetry (DLT-D20-S100).*

4.2 FINITE ELEMENT FORMULATION

In this section, the constitutive model used to simulate the failure behaviour of Sitka spruce DLT members fastened with CW dowels is presented. As part of the development of the three-dimensional model, a UMAT subroutine has

https://doi.org/10.52202/069179-0030

been developed to simulate the damage experienced in timber elements when subjected to stress under loading. The elastic component of the timber, CW dowels and steel plates follows the generalised Hooke's law. The material behaviour of the timber and CW dowels are assumed to be orthotropic with a stronger and stiffer response along the fibre direction and reduced properties perpendicular to the grain. The material properties for both the timber and CW are presented in Table 2. For simplicity, the radial and tangential directions of the timber are considered equal in this model. The subscript '*L*' and '*T*' represent the longitudinal and transverse materials directions for timber. E_L and E_T represent the elastic modulus in the longitudinal or parallel to the grain direction and the transverse or perpendicular to the grain direction, respectively. G_{LT} and G_{TT} are the shear moduli and v_{LT} and v_{TT} are the Poisson's ratios.

Similar to the elastic properties, the strength characteristics are also assumed to be directionally dependent. The values are presented in Table 2 with superscripts '*t*' and '*c*' which refer to the tension and compression, respectively. For example, $\sigma_L{}^t$ represents the value of the longitudinal failure stress when loaded in tension. The shear failure stress, τ_{LT} is also presented.

$$f_L = \sqrt{\frac{\varepsilon_{11}^t}{\varepsilon_{11}^c}(\varepsilon_{11})^2 + \left(\varepsilon_{11}^t - \frac{(\varepsilon_{11}^t)^2}{\varepsilon_{11}^c}\right)\varepsilon_{11}} > \varepsilon_{11}^t \qquad (1)$$

where

$$\varepsilon_{11}^t = \sigma_L^t/C_{11};\ \varepsilon_{11}^c = \sigma_L^c/C_{11} \qquad (2)$$

where *Cij* are the components of the elastic matrix in the undamaged state. When Eq. (1) is satisfied, the damage variable d_L is determined according to Eq. (3).

$$d_L = 1 - \frac{\varepsilon_{11}^t}{f_L} e^{(-C_{11}\varepsilon_{11}^t(f_L - \varepsilon_{11}^t)L_C/G_L)} \qquad (3)$$

where L_C and G_L are the characteristic element length and the fracture energy, respectively.

The corresponding equations for the perpendicular to the grain direction are produced similarly in Eqs. (4), (5) and (6),

$$f_T = \sqrt{\frac{\varepsilon_{22}^t}{\varepsilon_{22}^c}(\varepsilon_{22})^2 + \left(\varepsilon_{22}^t - \frac{(\varepsilon_{22}^t)^2}{\varepsilon_{22}^c}\right)\varepsilon_{22} + \left(\frac{\varepsilon_{22}^t}{\varepsilon_{12}^\tau}\right)^2(\varepsilon_{12})^2} > \varepsilon_{22}^t \qquad (4)$$

where

$$\varepsilon_{22}^t = \sigma_T^t/C_{22};\quad \varepsilon_{22}^c = \sigma_T^c/C_{22};\quad \varepsilon_{12}^\tau = \tau_{LT}^t/C_{44} \qquad (5)$$

When Eq. (4) is satisfied, the damage variable d_T is determined according to Eq. (6).

$$d_T = 1 - \frac{\varepsilon_{22}^t}{f_T} e^{(-C_{22}\varepsilon_{22}^t(f_T - \varepsilon_{22}^t)L_c/G_T)} \qquad (6)$$

The occurrence of damage is established when the elastic matrix is updated to form an effective elasticity matrix (C_d) which has terms reduced by including the two damage variables d_L and d_T as shown in Eq. (7).

$$C_d = \begin{bmatrix} (1-d_L)C_{11} & (1-d_L)(1-d_T)C_{12} & (1-d_L)C_{13} & 0 & 0 & 0 \\ & (1-d_T)C_{22} & (1-d_T)C_{23} & 0 & 0 & 0 \\ & & C_{33} & 0 & 0 & 0 \\ & Symmetric & & (1-d_L)(1-d_T)C_{44} & 0 & 0 \\ & & & & C55 & 0 \\ & & & & & C66 \end{bmatrix} \qquad (7)$$

G_T and G_L represent the fracture energies in the transverse and longitudinal directions, respectively and to improve convergence, a viscosity parameter, η is utilised in the user subroutine to regularise the damage variables and control the rate of damage.

The damage initiation criteria utilised in this model are based on the Hashin damage model which has been utilised in a series of studies to determine the failure behaviour of timber elements [27–31]. The damage initiation criteria are expressed in terms of strains and are treated differently for tension and compression strains however, one affects the other and if the strains are significant and cause partial or full damage (damage variable greater than zero) both tensile and compressive responses are affected. For example, damage in the longitudinal direction is initiated when the following criterion is achieved.

In the user subroutine, the stresses are then updated according to Eq. (8)

$$\sigma = C_d : \varepsilon \qquad (8)$$

The differentiation of the above equation is used to determine the Jacobian matrix as presented in Eq. (9).

$$\frac{\partial\sigma}{\delta\varepsilon} = C_d + \frac{\delta C_d}{\delta\varepsilon} : \varepsilon = C_d + \left(\frac{\delta C_d}{\delta d_T} : \varepsilon\right)\left(\frac{\delta d_T}{\delta f_T}\frac{\delta f_T}{\delta\varepsilon}\right) + \left(\frac{\delta C_d}{\delta d_L} : \varepsilon\right)\left(\frac{\delta d_L}{\delta f_L}\frac{\delta f_L}{\delta\varepsilon}\right) \qquad (9)$$

Furthermore, to improve the convergence, a viscosity parameter, η is utilised in the user subroutine to regularise the damage variables and control the rate of damage using the following Eqs (10) and (11).

$$\dot{d}_L^r = \frac{1}{\eta}(d_L - d_L^r) \qquad (10)$$

$$\dot{d}_T^r = \frac{1}{\eta}(d_T - d_T^r) \qquad (11)$$

where all parameters are as presented before but the superscript '*r*' indicates regularised and the accent '˙' indicates rate. The regularised damage variable is updated for each time step in the analysis.

https://doi.org/10.52202/069179-0030

4.3 MATERIAL DATA

The material data used in this model for the timber and the CW dowels are presented in Table 2. The steel plates are modelled as linear elastic material with an elastic modulus of 210 GPa and a Poisson's ratio of 0.3. The timber material is modelled as an orthotropic elastic material in Abaqus FEA software. The Sitka spruce material tested experimentally by O'Ceallaigh et al. [14–16] was graded to strength class C16. The standard EN 338 [17] provides a mean value of 8000 MPa for the elastic modulus of C16 timber in the longitudinal direction. The tangential elastic moduli (radial and tangential) directions were not measured experimentally; however, Bodig & Jayne [18] expressed a general relationship between the elastic modulus, E and shear modulus, G in the three material directions. Although these ratios are not without their inaccuracies, they are widely accepted for modelling the orthotropic properties of timber. The CW material properties presented in Table 2 are based on findings by O'Ceallaigh et al. [5,23]. Furthermore, a foundation zone was implemented within a 5 mm area surrounding each dowel home which accounts for reduced properties in this area. This approach is based on the foundation model proposed by Hong [32] which aims to account for the imperfect contact between the hole and fastener and also the reduction in strength due to the damage due to drilling to accommodate the CW dowels. Similar to Hong [32], both stiffness and yield properties are reduced. In this study, both stiffness and yield properties of timber are reduced to 20% [23].

Table 2: *FEM UMAT Material properties*

Property	Timber	CW Dowels	Unit
E_L	8000	13440	MPa
E_T	663	1075	MPa
G_{LT}	659	960	MPa
G_{TT}	66	96	MPa
ν_{LT}	0.038	0.48	-
ν_{TT}	0.558	0.35	-
σ_L^t	36	110.5	MPa
σ_L^c	40	110.5	MPa
σ_T^t	6	68	MPa
σ_T^c	9.6	68	MPa
τ_{LT}	6.9	5.9	MPa
G_T	10	30	N/mm
G_L	12	60	N/mm
η	0.0001	0.0001	-

The definition of the symbols and the notation has been presented in Section 0.

4.4 PARAMETRIC STUDY

In this study, Sitka spruce timber grown in Ireland is used as the primary structural material and the influence of a series of design parameters, namely, dowel diameter and dowel spacing, on the structural behaviour of a DLT beam is investigated. As part of the parametric study, three dowel diameters, 10 mm, 15 mm and 20 mm and three dowel spacing distances of 50 mm, 75 mm and 100 mm will be examined using a numerical model, once validated, to determine the structural behaviour. The naming convention of each specimen is presented in **Error! Reference source not found.**.

Table 3: *Numerical models and design parameters*

Numerical model Specimen	Dowel Diameter (mm)	Dowel Spacing (mm)
DLT-D10-S50	10	50
DLT-D15-S50	15	50
DLT-D20-S50	20	50
DLT-D10-S75	10	75
DLT-D15-S75	15	75
DLT-D20-S75	20	75
DLT-D10-S100	10	100
DLT-D15-S100	15	100
DLT-D20-S100	20	100

5 NUMERICAL RESULTS

The numerical model has been developed to simulate the load-displacement response with failure modes comprising a combination of dowel bending, dowel-timber embedment and tensile fracture of the bottom tensile laminate. This section presents the validation of the developed model against experimental results presented in Section 3 and then presents the parameter study investigating the influence of dowel diameter and spacing.

5.1 MODEL VALIDATION

The results of the numerical model are presented and compared to the experimental results in Figure 8. It can be seen that the numerically determined stiffness of the DLT beam matches that of the experimentally tested specimens. Typically, the simulated load-displacement behaviour of the DLT is in agreement with that observed experimentally, with linear elastic behaviour followed by a significant drop in the load-carrying capacity of the element.

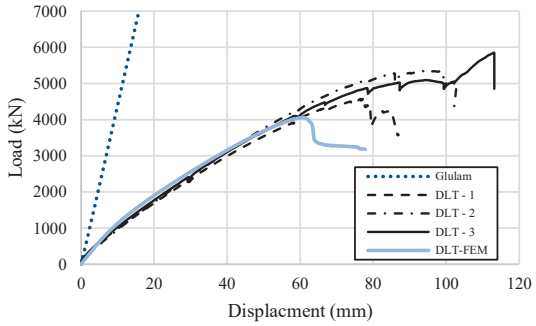

Figure 8. *Load-displacement behaviour of the 10 mm diameter dowel series*

Table 4: *Experimental results vs numerical model*

Member	F_{max} (kN)	U_{max} (mm)	Stiffness (N/mm^2)
DLT-1	4.57	76.6	1520
DLT-2	5.34	93.8	1588
DLT-3	5.85	113.2	1537
Mean	5.26	94.5	1548
DLT-FEM	4.06	61.03	1814.71
Perc. Diff.	26%	43%	16%

https://doi.org/10.52202/069179-0030

The maximum load, maximum displacement and stiffness of each beam are compared to the numerically simulated results in Table 4. The results show that the results are that conservative predictions are given for the maximum load and maximum displacement with percentage differences of 26% and 43%, respectively. In the case of stiffness, the numerically simulated results over-predict the stiffness that was observed experimentally. It is noted that the model does not provide a brittle rupture of the beam as was observed experimentally, and instead, the material that was damaged reduces in stiffness which mimics the failure of the material. This occurred experimentally in the tensile face of the DLT and was predicted in the zone in the numerical model. Furthermore, the damage observed in the dowels (Figure 6) and the stepped profile numerical model (Figure 9) were accurately captured by the model.

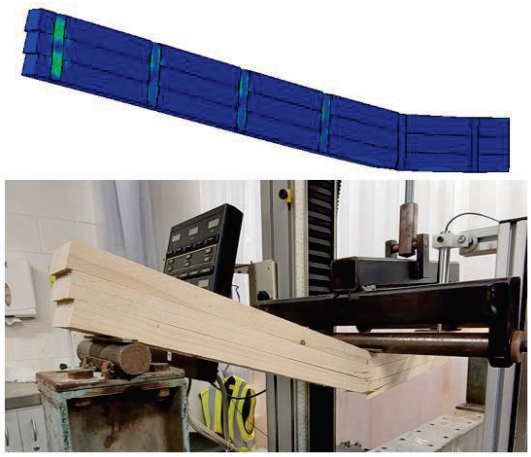

Figure 9: *FE vs experimental, tensile failure of bottom tensile laminate, and stepped profile from interlaminar slip.*

The model has demonstrated the ability to examine the local failure behaviour of the dowel/timber interaction with dowel bending and embedment at the dowel-timber interface and the load-displacement behaviour is in agreement with the experimental results.

5.2 PARAMETRIC STUDY RESULTS

In this section, the results of the numerical parametric study of the DLT specimens are presented. The load-displacement behaviour simulated by the numerical model is presented along with the maximum load (F_{max}) from each model, the displacement at maximum load (U_{max}) and the stiffness. The stiffness is determined on the linear proportion of the graph between 10% and 40% of the maximum load. These results are presented in Table 5 and the corresponding load-displacement graphs and presented in Figure 10, Figure 11, and Figure 12. In all cases, the numerically simulated curves are characterised by linear elastic behaviour until failure which comprised a combination of dowel bending, dowel-timber embedment and tensile fracture of the bottom tensile laminate.

Table 5: *Numerical model results*

Numerical Model Specimen	F_{max} (N)	U_{max} (mm)	Stiffness (N/mm^2)
DLT-D10-S50	4752	65.8	2292
DLT-D15-S50	4770	44.2	2913
DLT-D20-S50	3830	43.7	2503
DLT-D10-S75	4494	68.2	1984
DLT-D15-S75	4503	48.4	2731
DLT-D20-S75	3537	48.5	2395
DLT-D10-S100	4057	61.0	1815
DLT-D15-S100	4163	39.9	2705
DLT-D20-S100	3250	47.6	2338

The results presented in Figure 10, Figure 11, and Figure 12 are associated with DLT members with dowel diameters of 10 mm, 15 mm and 20 mm dowels, respectively. In each figure, a line indicated as 'Glulam' represents the theoretical stiffness of a glued beam with an elastic modulus of 9200 N/mm^2 to allow for comparison with the stiffness of the DLT members. In Figure 10, the influence of spacing on DLT members with a diameter of 10 mm can be observed and it is clear that decreasing the spacing between the 10 mm dowels has a positive impact on strength and stiffness. Reducing the spacing from 100 mm to 50 mm results in an increase in strength and stiffness of 17% and 26%, respectively.

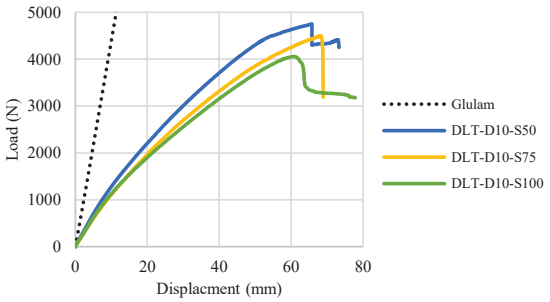

Figure 10. *Numerical load-displacement curves for specimens with 10 mm diameter dowels (D-10 Series).*

When the dowel diameter is increased to 15 mm, as seen in Figure 11, an improvement in strength and stiffness was observed for each dowel spacing studied. The influence of dowel spacing was not as significant as was observed for the 10 mm dowels with increases of 14% and 7% in strength and stiffness, respectively.

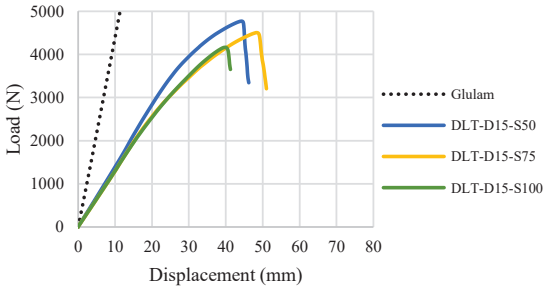

Figure 11. *Numerical load-displacement curves for specimens with 15 mm diameter dowels (D-15 Series).*

https://doi.org/10.52202/069179-0030

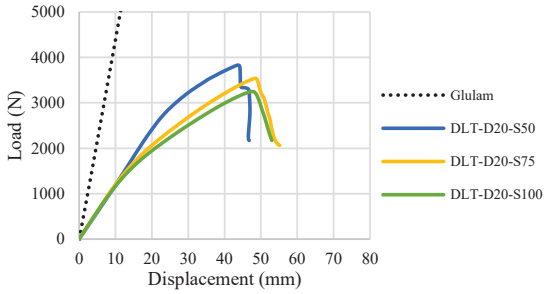

Figure 12. *Numerical simulated load-displacement curves for specimens with 20 mm diameter dowels (D-20 Series).*

Finally, for the 20 mm dowels, presented in Figure 12, contrasting load-displacement behaviour was observed. Increasing the dowel diameter to 20 mm has a negative influence on strength and stiffness. The results indicate that load-displacement behaviour is governed by the timber substrate with limited dowel/timber interaction and further studies should examine the effect for larger cross-sections.

The influence of dowel spacing for all specimens studied can be seen in Figure 13 and Figure 14. In Figure 13, it can be seen that the 50 mm spacing provided the highest loads for the 10 mm and 15 mm dowel diameters but this was not the case for the 20 mm dowels. This may be an issue with reduced edge distances and may not be the case for larger cross-sections.

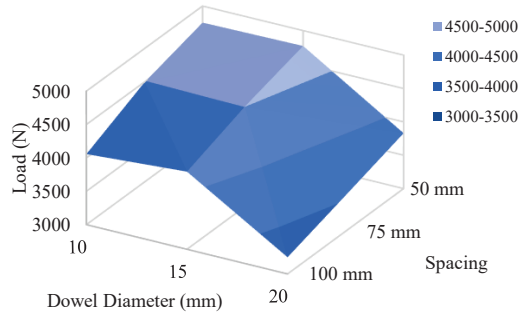

Figure 13. *The influence of dowel diameter and dowel spacing on maximum load (F_{max}).*

In Figure 14, the influence of dowel diameter and spacing on the observed stiffness for all specimens studied can be seen. It is clear that as the dowel diameter is increased from 10 mm to 15 mm, there was a positive influence on the stiffness of the DLT beam. The maximum stiffness was observed for the 15 mm CW dowels with a spacing of 50 mm. The stiffness of the 20 mm dowels did not perform as expected. While there was a positive increase in stiffness when increasing the dowel diameter from 10 mm to 15 mm, reduced stiffness was observed for dowel diameters of 20 mm, regardless of dowel spacing. The results of the numerical model indicated that the timber substrate was subjected to relatively high stress concentration adjacent to the dowel holes in the tension zone of the DLT members. This would indicate that the edge spacing criterion needs to be further examined.

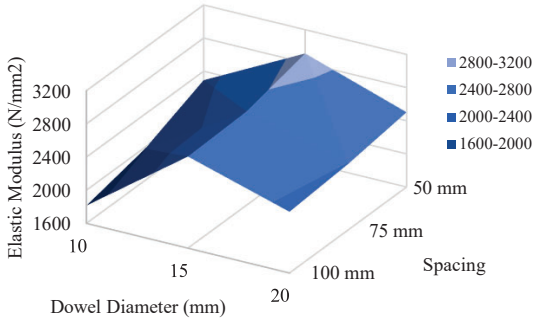

Figure 14. *The influence of dowel diameter and dowel spacing on elastic modulus.*

6 CONCLUSIONS

The feasibility of manufacturing DLT elements from Irish-grown Sitka spruce connected with CW dowels has been examined through experimental testing. A series of experimental tests have demonstrated relatively similar load-displacement behaviour in all specimens for the given dowel diameter (10 mm) and spacing (100 mm). The results have demonstrated that significant loads can be achieved through dowel laminating technology using Irish-grown timber which creates a value-added product with improved environmental credentials compared to adhesively bonded wood products. It is noted that the use of dowels instead of adhesive results in reduced capacity and stiffness for equivalent section sizes but this work has contributed to a better understanding of the behaviour for safe design in the future. There is also a significant opportunity to further refine the design and optimise this for increased structural capacity and stiffness.

A numerical model is presented and has been validated against the experimental results. The results show that the numerical model shows good agreement with the experimental results and the failure modes have also been adequately simulated by the numerical model. A parametric study has been carried out and the numerical results of DLT members connected using CW dowels have been presented for dowel diameters of 10 mm, 15 mm, and 20 mm with spacings arrangements of 50 mm, 75 mm and 100 mm. Typically, increasing the dowel diameter and reducing the dowel spacing have a positive influence on the strength and stiffness of the DLT members. This was not the case for the 20 mm dowels examined in this study and is believed to be due to edge spacing criteria which required further attention.

ACKNOWLEDGEMENT

The authors would like to express their gratitude for the support and funding of the Department of Agriculture, Food and the Marine's Competitive Research Funding Programmes, Project Ref: 2019R471 (MODCONS).

REFERENCES

[1] StructureCraft, Dowel Laminated Timber (DLT) - Design and Profile Guide, StructureCraft, USA, 2019.

[2] A. Thoma, D. Jenny, M. Helmreich, A. Gandia, F.

Gramazio, M. Kohler, Cooperative Robotic Fabrication of Timber Dowel Assemblies, in: Res. Cult. Archit., Birkhäuser, Berlin, Boston, 2019: pp. 77–88. doi:10.1515/9783035620238-008.

[3] I. El-Houjeyri, V.D. Thi, M. Oudjene, M. Khelifa, Y. Rogaume, A. Sotayo, Z. Guan, Experimental investigations on adhesive free laminated oak timber beams and timber-to-timber joints assembled using thermo-mechanically compressed wood dowels, Constr. Build. Mater. 222 (2019) 288–299.

[4] S. Mehra, C. O'Ceallaigh, A. Sotayo, Z. Guan, A.M. Harte, Experimental investigation of the moment-rotation behaviour of beam-column connections produced using compressed wood connectors, Constr. Build. Mater. 331 (2022) 127327. doi:10.1016/j.conbuildmat.2022.127327.

[5] C. O'Ceallaigh, P. McGetrick, A.M. Harte, The Structural Behaviour of Compressed Wood Manufactured using Fast-grown Sitka Spruce, in: WCTE 2021 - World Conf. Timber Eng., Santiago, Chile, 2021.

[6] CEN, EN 408. Timber structures - Structural timber and glued laminated timber - Determination of some physical and mechanical properties, Comité Européen de Normalisation, Brussels, Belgium, 2012.

[7] W. Plowas, T. Bell, R. Hairstans, J.B. Williamson, Understanding the compatibility of UK resource for dowel laminated timber construction, TH Build. Constr. (2015) 1–12.

[8] C. O'Loinsigh, M. Oudjene, E. Shotton, A. Pizzi, P. Fanning, Mechanical behaviour and 3D stress analysis of multi-layered wooden beams made with welded-through wood dowels, Compos. Struct. 94 (2012) 313–321. doi:10.1016/j.compstruct.2011.08.029.

[9] C. O'Loinsigh, M. Oudjene, H. Ait-Aider, P. Fanning, A. Pizzi, E. Shotton, E.M. Meghlat, Experimental study of timber-to-timber composite beam using welded-through wood dowels, Constr. Build. Mater. 36 (2012) 245–250. doi:10.1016/j.conbuildmat.2012.04.118.

[10] A. Sotayo, D. Bradley, M. Bather, P. Sareh, M. Oudjene, I. El-Houjeyri, A.M. Harte, S. Mehra, C. O'Ceallaigh, P. Haller, S. Namari, A. Makradi, S. Belouettar, L. Bouhala, F. Deneufbourg, Z. Guan, Review of state of the art of dowel laminated timber members and densified wood materials as sustainable engineered wood products for construction and building applications, Dev. Built Environ. 1 (2020) 100004. doi:10.1016/j.dibe.2019.100004.

[11] M. Oudjene, M. Khelifa, C. Segovia, A. Pizzi, Application of numerical modelling to dowel-welded wood joints, J. Adhes. Sci. Technol. 24 (2010) 359–370. doi:10.1163/016942409X12541266699473.

[12] Z. Guan, A. Sotayo, M. Oudjene, I. El Houjeyri, A. Harte, S. Mehra, P. Haller, S. Namari, S. Belouettar, F. Deneufbourg, Development of Adhesive Free Engineered Wood Products – Towards Adhesive Free Timber Buildings, in: Proc. WCTE 2018 World Conf. Timber Eng. Seoul, Rep. Korea, August 20-23, 2018, 2018.

[13] ETA-13/0785, European Technical Approval. Solid wood slab element - element of dowel jointed timber boards to be used as a structural elements in buildings, ETA-Denmark, Nordhavn, Denmark, 2013.

[14] C. O'Ceallaigh, K. Sikora, D. McPolin, A.M. Harte, An investigation of the viscoelastic creep behaviour of basalt fibre reinforced timber elements, Constr. Build. Mater. 187 (2018) 220–230. doi:10.1016/j.conbuildmat.2018.07.193.

[15] C. O'Ceallaigh, K. Sikora, D. McPolin, A.M. Harte, Modelling the hygro-mechanical creep behaviour of FRP reinforced timber elements, Constr. Build. Mater. 259 (2020). doi:10.1016/j.conbuildmat.2020.119899.

[16] C. O'Ceallaigh, An Investigation of the Viscoelastic and Mechano-sorptive Creep Behaviour of Reinforced Timber Elements, PhD Thesis, National University of Ireland Galway, 2016.

[17] CEN, EN 338. Structural timber - Strength classes, Comité Européen de Normalisation, Brussels, Belgium, 2016.

[18] J. Bodig, B.A. Jayne, Mechanics of Wood Composites. Reprinted edition, Kreiger Publishing Company. USA, 1993.

[19] M. Conway, C. O'Ceallaigh, S. Mehra, A.M. Harte, Reinforcement of Timber Elements in Compression Perpendicular to the Grain using Compressed Wood Dowels, in: Civ. Eng. Res. Ireland, CERI 2020. Cork Inst. Technol. 27-28 August, 2020: pp. 319–324. doi:https://doi.org/10.13025/sbeg-3p91.

[20] S. Mehra, I. Mohseni, C. O'Ceallaigh, Z. Guan, A. Sotayo, A.M. Harte, Moment-rotation behaviour of beam-column connections fastened using compressed wood connectors, in: SWST 62 Nd Int. Conv. Renew. Mater. Wood-Based Bioeconomy, 2019: p. 2019.

[21] C. O'Ceallaigh, M. Conway, S. Mehra, A.M. Harte, Numerical Investigation of Reinforcement of Timber Elements in Compression Perpendicular to the Grain using Densified Wood Dowels, Constr. Build. Mater. 288 (2021). doi:10.1016/j.conbuildmat.2021.122990.

[22] M. Conway, A.M. Harte, S. Mehra, C. O'Ceallaigh, Densified Wood Dowel Reinforcement of Timber Perpendicular to the Grain: A Pilot Study, J. Struct. Integr. Maint. 6 (2021) 177–186. doi:10.1080/24705314.2021.1906090.

[23] C. O'Ceallaigh, I. Mohseni, S. Mehra, A.M. Harte, Numerical Investigation of the Structural Behaviour of Adhesive Free Connections Utilising Modified Wood, in: WCTE 2021-World Conf. Timber Eng., Chile, 2021.

[24] S. Namari, L. Drosky, B. Pudlitz, P. Haller, A.

https://doi.org/10.52202/069179-0030

Sotayo, D. Bradley, S. Mehra, C. O'Ceallaigh, A.M. Harte, I. El-houjeyri, M. Oudjene, Z. Guan, Mechanical properties of compressed wood, Constr. Build. Mater. 301 (2021). doi:10.1016/j.conbuildmat.2021.124269.

[25] K. Jung, A. Kitamori, K. Komatsu, Evaluation on structural performance of compressed wood as shear dowel, Holzforschung. 62 (2008) 461–467. doi:10.1515/HF.2008.073.

[26] S. Mehra, A.M. Harte, A. Sotayo, Z. Guan, C. O'Ceallaigh, Experimental investigation on the effect of accelerated ageing conditions on the pull-out capacity of compressed wood and hardwood dowel type fasteners, Holzforschung. (2021).

[27] H. Valipour, N. Khorsandnia, K. Crews, A. Palermo, Numerical modelling of timber/timber-concrete composite frames with ductile jointed connection, Adv. Struct. Eng. (2016). doi:10.1177/1369433215624600.

[28] B. Kawecki, J. Podgórski, Numerical analysis and its laboratory verification in bending test of glue laminated timber pre-cracked beam, Materials (Basel). 16 (2019) 1–15. doi:10.3390/ma12060955.

[29] F. Portioli, R. Marmo, C. Ceraldi, R. Landolfo, Numerical modeling of connections with timber pegs, in: 11th World Conf. Timber Eng. 2010, WCTE 2010, 2010: pp. 1881–1886.

[30] N. Khorsandnia, H.R. Valipour, K. Crews, Nonlinear finite element analysis of timber beams and joints using the layered approach and hypoelastic constitutive law, Eng. Struct. 46 (2013) 606–614. doi:10.1016/j.engstruct.2012.08.017.

[31] M. Chybiński, Ł. Polus, Experimental and numerical investigations of aluminium-timber composite beams with bolted connections, Structures. 34 (2021) 1942–1960. doi:10.1016/j.istruc.2021.08.111.

[32] J.-P. Hong, Three-Dimensional Nonlinear Finite Element Model for Single and Multiple Dowel-type Wood Connections, PhD Thesis, The University of British Columbia, 2007.